Biogeochemistry (2016) 129:37–51
DOI 10.1007/s10533-016-0218-4

Vertical distribution of carbon and nitrogen stable isotope ratios in topsoils across a temperate rainforest dune chronosequence in New Zealand

Melanie Brunn · Leo Condron · Andrew Wells · Sandra Spielvogel · Yvonne Oelmann

Received: 19 November 2015 / Accepted: 11 May 2016 / Published online: 26 May 2016

Abstract Chronosequences can provide valuable insights into carbon (C) and nitrogen (N) dynamics across natural gradients with C and N stable isotopes serving as powerful tool investigating these dynamics. We studied changes in $\delta^{13}C$ and $\delta^{15}N$ values in litter, organic layer and mineral soil on dunes across the Haast chronosequence (New Zealand), which spans 120 to 2870 years of pedogenesis beneath a temperate rainforest. Decomposition was approximated from linear regression slopes between C concentrations and $\delta^{13}C$ values and termed $beta_C$. Similarly we calculated $beta_N$ values to test the relationship between vertical N decrease and $\delta^{15}N$ increase. Decreasing $\delta^{13}C$ values of litter with age suggests a physiological response of plants to decreased litter N concentrations. A decrease of litter $\delta^{15}N$ in the early succession stages and a second decline after 1300 years indicates reduced N_2 fixation. $Beta_C$ values increased during early ecosystem development and at old sites, and were lowest at the intermediate stages (1500 years), which suggests decomposition did not decrease constantly with time. $Beta_N$ values were lowest at the youngest site and increased within the first 200 years, likely because litter as the uppermost part of the vertical depth profile reflected an increased supply of N depleted in ^{15}N provided by fungi. We found relations between $beta_C$ and $beta_N$ values suggesting that there might be shared processes shaping $\delta^{13}C$ and $\delta^{15}N$ vertical depth profiles, e.g. microbial cycling, transport or sorption.

Keywords $\delta^{13}C$ and $\delta^{15}N$ depth profile · Natural abundance stable isotopes · N_2 fixation · Nutrient limitation · Organic layer · Organic matter decomposition

Responsible Editor: Stephen Porder.

Electronic supplementary material The online version of this article (doi:10.1007/s10533-016-0218-4) contains supplementary material, which is available to authorized users.

M. Brunn (✉) · Y. Oelmann
Geoecology, University of Tuebingen, Ruemelinstraße 19-23, 72070 Tuebingen, Germany
e-mail: melanie.brunn@uni-tuebingen.de

L. Condron · A. Wells
Faculty of Agriculture and Life Sciences, Lincoln University, Lincoln, New Zealand

S. Spielvogel
Institute of Geography, University of Bern, Bern, Switzerland

Introduction

Chronosequences provide unique opportunities to investigate carbon (C) and nitrogen (N) dynamics in natural ecosystems. Environmental and biological changes during ecosystem development are considered an important driver of C stabilization in soils (Jones et al. 2015; Schmidt et al. 2011) which

profoundly affects atmospheric carbon dioxide concentrations (Stockmann et al. 2013). For example, in boreal systems with slow decomposition, old soils sequestered more C than younger soils, caused by the accumulation of an organic layer (Clemmensen et al. 2013). Stable isotopes of carbon ($\delta^{13}C$) and nitrogen ($\delta^{15}N$) can be used as indirect indicators of biogeochemical patterns and processes across chronosequences (Craine et al. 2015; Högberg 1997). During biogeochemical reactions, isotopic fractionation occurs, i.e. a discrimination of heavier isotopes that leave the reactant enriched and the product isotopically depleted (Hobbie and Högberg 2012). For instance, isotopic ratios served to assess plant N nutrition (Hyodo et al. 2013; Unkovich 2013), C and N transfer to and by mycorrhizal fungi (Clemmensen et al. 2013; Hobbie and Högberg 2012), decomposition (Acton et al. 2013; Brunn et al. 2014; Garten 2006; Guillaume et al. 2015) or interrelations between above and belowground processes (Hobbie and Ouimette 2009; Hyodo and Wardle 2009; Menge et al. 2011). Despite the complexity of the C and N cycle, interpretation of C and N isotopes in plants, soil and depth profiles can help to elucidate key aspects and processes that dominate the C and N cycle in particular ecosystems.

Ecosystem and soil development across chronosequences can be defined in a progressive phase after initial disturbance, in a phase of maximal biomass in which the ecosystem stabilizes and in a retrogressive phase, where the ecosystem undergoes declines in productivity and nutrient cycling; trends that have been observed along chronosequences around the world (Peltzer et al. 2010; Wardle et al. 2004). Early in primary succession, primary production is commonly limited by N availability (Vitousek 2004; Vitousek and Howarth 1991), which may progress to phosphorus (P) limitation in extremely old and/or highly weathered soils (Vitousek and Farrington 1997; Walker and Syers 1976). Changes in C and N stocks and cycling accompany these biogeochemical shifts, and may influence the isotopic signatures of plants and soils (Martinelli et al. 1999).

For example, litter $\delta^{13}C$ values in boreal forest chronosequences in Sweden increased with proceeding time (Hyodo et al. 2013; Hyodo and Wardle 2009). Foliar morphological adaption to lower nutrient availability at late stages of pedogenesis, i.e. increased internal resistance of CO_2 diffusion through the development of thicker and smaller leaves was supposed. This adaption is comparable to water stress effects on plants that equally reduces the stomatal conductance and results in higher $\delta^{13}C$ values due to closed stomata (Farquhar et al. 1989). Similarly, according to positive relations between foliar N concentrations and $\delta^{13}C$ values (Guehl et al. 1995; Körner and Diemer 1987; Vitousek et al. 1990), $\delta^{13}C$ values should increase with increasing N and therefore with time across chronosequences.

In contrast to foliar and litter $\delta^{13}C$ values, which typically is interpreted as an integrator of water stress, $\delta^{15}N$ values have been used to infer N input and loss pathways, as well as overall N availability (Craine et al. 2015; Högberg 1997). Specifically, $\delta^{15}N$ of litter reflects the fraction of N incorporated from dinitrogen (N_2) fixation, as well as isotopic enrichment of the available soil N pool due to fractionating losses that preferentially remove ^{14}N (e.g. denitrification) (Houlton and Bai 2009; Houlton et al. 2006). Due to the negligible fractionation during nutrient retranslocation before leaf abscission (Garten et al. 2011; Menge et al. 2011), $\delta^{15}N$ values in litter layer of soils can reflect N sources and their transformation by N cycling processes. Across chronosequences, deposition or bedrock material are comparable and should not affect variations in litter $\delta^{15}N$ values, while N loss and all other forms of N input may change. However, to compare chronosequences from different sites with each other, all N input values have to be considered, making chronosequences of each site specific in its isotopic signature. For example, low N deposition and less N from bedrock in early phases of ecosystem development can generate systems with strong dependence on N_2 fixation (Menge and Hedin 2009; Vitousek and Howarth 1991). The high energy costs of N_2 fixation make it unlikely to persist if soil N availability is high compared to the utilization of other N forms (Andrews et al. 2011; Vitousek and Howarth 1991). However, contrasting trends with a decoupling of N_2 fixation and N availability in soil were also documented (Menge and Hedin 2009; Reed et al. 2011). Since litter $\delta^{15}N$ values converge to atmospheric isotopic signatures at sites where biological N_2 fixation dominates (Unkovich 2013) and e.g., N supplied by fungi results in ^{15}N depleted litter (Hobbie and Ouimette 2009), litter $\delta^{15}N$ values can help to indicate the dominating N source used by plants.

The uppermost litter layer contains more C and N than mineral soil below and this vertical decrease in C and N concentrations is associated with an increase in $\delta^{13}C$ and $\delta^{15}N$ values, i.e. organic matter (OM) becomes enriched lower in the soil (Billings and Richter 2006; Brunn et al. 2014; Hobbie and Ouimette 2009; Nadelhoffer and Fry 1988). In addition to several mechanisms and processes driving vertical isotopic changes, the accumulation of ^{13}C and ^{15}N enriched compounds from microbial products or microbial cells itself are supposed as important parameters (Billings and Richter 2006; Dijkstra et al. 2006; Lerch et al. 2011). Vertical isotopic patterns in soils have been described by enrichment factors corresponding to the isotopic difference from litter to mineral soil (Krull et al. 2002) or by plotting logarithmized ($\log_{10}x$) element concentration in OM against its isotopic signature (Acton et al. 2013; Brunn et al. 2014; Garten 2006; Guillaume et al. 2015). In the latter, slopes of linear regressions (indicated as $beta_C$ values) between logarithmized C concentrations and the according isotopic ratios served to approximate decomposition. $Beta_C$ values could therefore be a valuable tool to assess changes of C processing during ecosystem and soil development.

In addition to the vertical enrichment of ^{13}C, a similar enrichment of ^{15}N can develop in topsoils (Craine et al. 2015; Hobbie and Ouimette 2009; Wallander et al. 2009). Likewise, $beta_N$ values can be calculated by means of linear regressions between logarithmized N concentrations and according $\delta^{15}N$ values. Similar relations were compiled by Hobbie and Ouimette (2009) and the authors emphasized the importance of mycorrhizal fungi in controlling vertical $\delta^{15}N$ depth trends. Fractionation against ^{15}N during N transfer by mycorrhizal fungi to host plants is suggested, resulting in ^{15}N depleted litter and ^{15}N enriched OM in mineral soil (Hobbie and Ouimette 2009). The vertical enrichment in ^{15}N between litter and mineral soil was found to vary strongly, with ectomycorrhizal (EM) systems *c.* doubling the enrichment in ^{15}N compared to systems dominated by arbuscular mycorrhiza (AM) (Hobbie and Ouimette 2009). Mycorrhizal associations inconstantly shifted with time across chronosequences (Dickie et al. 2013) with strong host specificity (Martinez-Garcia et al. 2015). For example, while boreal chronosequences are supposed to lack a stage with AM, EM plants are absent across sequences in Hawaii (Dickie et al. 2013). Chronosequences in New Zealand are potentially able to host both mycorrhiza types. However, the Franz Josef chronosequence (*c.* 200 km north of Haast) does not harbor EM plant species (Dickie et al. 2013) that are present at the late stages of the Haast chronosequence (Turner et al. 2012b).

In this study, we aimed to contribute to a better understanding of C and N dynamics with providing stable C and N isotope data in high resolution of topsoils during pedogenesis and ecosystem development. We investigated *c.* 2870 years across the well established Haast chronosequence (Eger et al. 2011; Jangid et al. 2013; Turner et al. 2012a, b, 2014) located on a well drained sandy dune substrate with fast podzolisation (Turner et al. 2012b) on New Zealand's South Island. Our objectives were to unravel whether (i) $\delta^{13}C$ and $\delta^{15}N$ values in litter and (ii) vertical shifts of $\delta^{13}C$ and $\delta^{15}N$ values with soil depth change with soil age across a soil chronosequence under superhumid climate conditions.

Previous studies showed increasing nutrient limitation across the Haast chronosequence (Turner et al. 2012a) and abundances of bacterial taxa closely related to heterotrophic diazotrophs (Jangid et al. 2013). Therefore, we hypothesized (1) that litter $\delta^{13}C$ values increase with proceeding ecosystem development and pedogenesis, similarly to $\delta^{13}C$ values in boreal chronosequences and (2) that $\delta^{15}N$ values of litter are close to the isotopic signature of atmospheric N_2 due to the high contribution of biological N_2 fixation at Haast. Conforming to the retrogressive model which suggests declines in ecosystem productivity, decomposition and nutrient cycling (Peltzer et al. 2010), we hypothesized (3) that $beta_C$ values, as a measure of decomposition, decrease with proceeding time. According to the possible shift in mycorrhizal communities with time, i.e. AM to EM due to host specificity inferred from shifts in tree species (Turner et al. 2012b), we hypothesized (4) that differences between $\delta^{15}N$ values of litter and mineral soil OM increase with time resulting in increasing $beta_N$ values.

Materials and methods

Sampling site

The Haast coastal foredune progradation dune ridge system has formed under temperate humid climate

(mean annual temperature = 11.3 °C, mean annual precipitation = 3455 mm) at the West Coast of New Zealand's South Island (43°53′S, 169°3′E). The chronosequence features comparable parent material with 88.7 ± 2.8 % sand, 8.0 ± 2.1 % silt and 3.5 ± 0.5 % clay content (Turner et al. 2012a), negligible human disturbance and low atmospheric N deposition (0.9–1.5 kg N ha^{-1} $year^{-1}$) (Galloway et al. 2004; Menge et al. 2011). Dune ridges form a slightly undulating topography (<5–20 m a.s.l.) with overall extension *c.* 5 km inland and soils developing from Arenosol to Podzol (Turner et al. 2012a). The whole formation covers a time of *c.* 6000 years and was extensively described by Wells and Goff (2007) and Turner et al. (2012a).

Sampling and sample preparation

We collected five replicate samples from litter, organic layer and mineral soil on 11 dune ridges (landward direction) in March 2013, resulting in 55 profiles covering a time span from *c.* 120 to *c.* 2870 years (Table 1). Soil samples were collected by a root auger (Eijkelkamp Agrisearch Equipment BV, Netherlands) to a depth of 10 cm of the mineral soil. After removal of soil cores (diameter of 8 cm), we cut mineral soil into 1 cm depth sections. Organic layers were collected as litter (Oi horizon) and organic (Oe and Oa horizons) layers. At some sites, thick roots restricted the depth which could be sampled, resulting in a sampling depth of 7 cm at dune stage 0 (B), 8 cm at dune stages 0 (A and D), 3 (A), 4 (B) and 5 (B) and 9 cm for two replicates of the dune stage 0 (C and E).

All samples were oven dried at 60 °C and visible roots and parts of green moss that survived drying procedure were carefully removed. The dried litter and organic layer samples were ground in a shredder (Retsch SM 2000). Dried mineral soil samples were sieved <2 mm. Aliquots and those of the shredded litter and organic layer samples were ground and homogenized using a Planetary Ball Mill PM 200 (Retsch, Germany).

Laboratory analysis, calculations and statistics

Elemental and isotopic measurements

Carbon and nitrogen concentrations were determined with an Elemental Analyzer (Isotope Cube, Elementar, Hanau, Germany). Since all soil samples were strongly acidic (Turner et al. 2012a) and free of carbonate (verified by means of hydrochloric acid addition to finely ground mineral soil samples), measured total C concentration equals the organic C

Table 1 Sampling sites description with dune age (B.P.), dating method, depth of the organic horizons (cm) (=Oi, Oe and Oa horizons) with standard errors and letters representing significant differences between the dune stages

Dune stage	Dune age (years B.P.)[a]	Dating method	Depth of the organic horizons (cm)
0[b]	120	Estimated	1.4 ± 0.5c
1[b]	187	Tree rings	1.0 ± 0.3c
2	296	Tree rings	3.8 ± 1.4bc
3	398	Tree rings	4.6 ± 0.5b
4	523	Tree rings	2.4 ± 0.2bc
5	603	Tree rings	3.4 ± 1.2bc
6[b]	793	Tree rings	3.0 ± 0.9bc
7	1310	Estimated	11.6 ± 2.5abc
8	1830	Estimated	26.2 ± 8.6abc
9	2350	Estimated	29.2 ± 3.8a
10	2870	Estimated	18.2 ± 3.3abc

[a] Dates from year of sampling (2013); ages of dune stages 1–6 from Wells and Goff (2007) and Turner et al. (2012a), (b) and stages 7–10 estimated by assuming an equal number of years (c. 520 years) between each dune stage

[b] Dunes for these stages were less pronounced on the north side of the river therefore, dunes occurring on a parallel system on the south side of the river were sampled

concentration. Stable isotope ratios were analyzed by coupled isotope ratio mass spectrometry (IRMS) (Isoprime 100, Isoprime, Manchester, England). Results are given in delta notation as $\delta^{13}C$ for C and $\delta^{15}N$ for N stable isotopes in ‰: (Eq. 1)

$$\delta^{13}C, \delta^{15}N[‰] = \left[\frac{R_{sample}}{R_{standard}} - 1\right] \times 1000, \quad (1)$$

where R represents the $^{13}C/^{12}C$ or the $^{15}N/^{14}N$ ratio, respectively. We used IAEA-CH-3, IAEA-CH-6 and IAEA-600 for normalization of measured $\delta^{13}C$ values (in $‰_{VPDB}$) and USGS25, IAEA-N-1 and IAEA-N-2 for normalization of measured $\delta^{15}N$ values (in $‰_{Air}$). Measurement precision of IRMS analyses based on routine measurements of interspersed samples per 15 samples of sulfanilic acid (Merck KGaA, Germany) during the measurement period was ±0.1 ‰ ($n = 53$) for $\delta^{13}C$ and ±0.2 ‰ ($n = 52$) for $\delta^{15}N$. This analytical uncertainty was less than the expected natural variability. Mean difference of duplicate measurement for $\delta^{13}C$ values ($n = 112$) of the organic horizons and mineral soil samples was 0.08 ‰ and for $\delta^{15}N$ values ($n = 53$) 0.07 ‰.

Calculations and statistical analysis

Linear regression analyses determined the patterns of isotopic changes within soil profiles. We regressed $\log_{10}x$-transformed element concentrations [$\log_{10}$ (g C kg^{-1})] or [$\log_{10}$ (10^{-1}g N kg^{-1})] (=x) and their according stable isotope values [$\delta^{13}C$] or [$\delta^{15}N$] (= y) of the depth intervals (organic layers and mineral soil) (Acton et al. 2013; Brunn et al. 2014; Garten 2006). Different units for the logarithmized C and N concentrations resulted in positive values on the *x*-axis. The absolute values of the slopes were termed beta and referred to as $beta_C$ and $beta_N$, respectively.

In addition to beta values, we used vertical isotopic differences to describe vertical changes in C ($\Delta^{13}C$) and N stable isotopes ($\Delta^{15}N$) from litter to mineral soil. There was spatial variation in the depth and thickness of soil horizons between dune stages, e.g. a soil horizon at 10 cm soil depth of a given location corresponds to a slightly deeper or shallower depth as compared to the neighboring sampling site. We tried to account for this by using maximum difference in profiles instead of the difference between the litter layer and mineral soil at 10 cm soil depth to best represent the vertical changes in $\delta^{13}C$ and $\delta^{15}N$ values. The difference between maximum $\delta^{13}C_{Max}$ or $\delta^{15}N_{Max}$ (isotopic signature of the mineral soil) and minimum values $\delta^{13}C_{Min}$ or $\delta^{15}N_{Min}$ (isotopic signature of the litter) of each profile was calculated using equation [2] for C and [3] for N values:

$$\Delta^{13}C = \delta^{13}C_{Max} - \delta^{13}C_{Min} \quad (2)$$

$$\Delta^{15}N = \delta^{15}N_{Max} - \delta^{15}N_{Min} \quad (3)$$

Linear regression analyses were used to quantify the impact of soil age on variables. We assessed trends across the overall chronosequence as well as in singles phases, i.e. the early phase (stages 0–2), the intermediate phase (stages 3–6) and the late phase (stages 7–10). Since these phases potentially do not cover the changes of variables with time in between these phases, we additionally provide two tables containing mean ± SE values of variables in the supplemental material with results from one-way ANOVA post hoc tests showing differences between the stages (Tables S1, S2). In case of homogeneous variances, we used a post hoc Tukey test. In case of heteroscedasticity, a Games-Howell test was conducted. In addition to this we applied matched pairs t tests (in case of homogeneity of variances) or Welch's *t*-tests (in case of heteroscedasticity) for the comparison of beta values, proportions of explained variations and $\Delta^{13}C$ or $\Delta^{15}N$ values. Autocorrelation of data was tested by the Durbin–Watson test and reconciled with critical values for the Durbin–Watson test provided by Savin and White (1977). Only non-autocorrelated data were evaluated. The level of significance was set to $P \leq 0.05$ in all tests. Probability of fit to normal distribution was tested by Kolmogorov–Smirnov tests.

Results

Element concentrations, C: N ratios and isotopic signatures in litter, organic layer and mineral soil with proceeding pedogenesis

With increasing soil depth, average C concentration in OM decreased from 338.2 ± SE 41.4 g C kg^{-1} in litter to 21.9 ± 1.2 g C kg^{-1} in mineral soil, while $\delta^{13}C$ values increased from −29.9 ± 0.9 $‰_{VPDB}$ to −28.2 ± 0.6 ‰ (Fig. 1). Similarly, average N

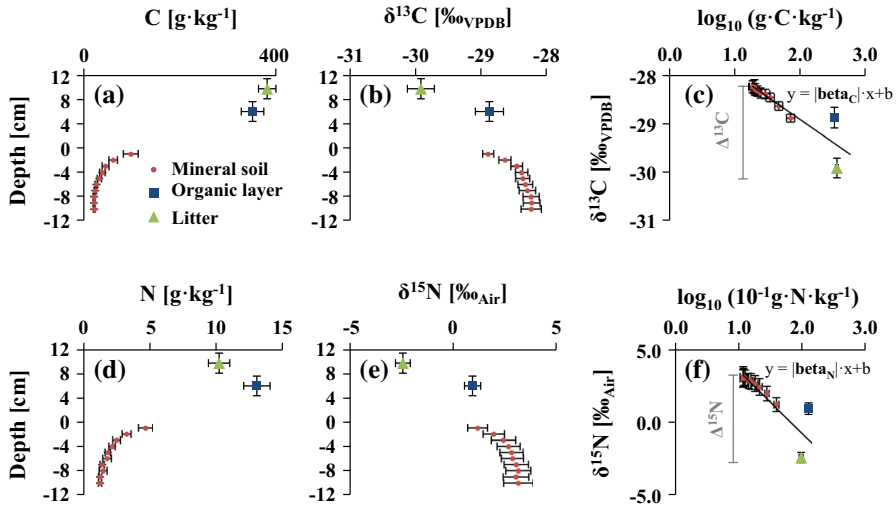

Fig. 1 Mean ± SE C (**a**) and N concentrations (g kg^{-1}) (**d**) and $\delta^{13}C$ ($‰_{VPDB}$) and **b** $\delta^{15}N$ values ($‰_{Air}$) **e** with depth (cm) across all dune stages ($n = 11$, except the organic layer: $n = 4$) showing a vertical decrease in C and N concentrations and an increase in $\delta^{13}C$ and $\delta^{15}N$ values. Figures on the *right* represent relations between $\log_{10}$ (g C kg^{-1}) and $\delta^{13}C$ values (**c**) or $\log_{10}$ (10^{-1}·g·N·kg^{-1}) and $\delta^{15}N$ values (f) of which beta values can be derived. Litter layer (Oi layer) values depicted as triangles ($n = 11$), organic layers (Oe and Oa layer) as squares ($n = 4$). Organic layers occur from stage 7 on (soil age > 1300 years) and are not present in the stages before. Depths of litter and organic layers as mean ± SE in cm. *Error bars* represent two standard errors

concentration decreased vertically from 12.3 ± 1.3 g N kg^{-1} to 1.3 ± 0.1 g N kg^{-1}, while $\delta^{15}N$ values increased from −2.4 ± 1.5 $‰_{Air}$ to 3.2 ± 2.7 ‰ (Fig. 1). Litter and organic layer thickness (Oi, Oe and Oa horizon) increased with time across the chronosequence ($P < 0.001$; $r = 0.745$) with development of a distinguishable organic layer (Oe and Oa horizon) from stage 7 onwards. Mean thickness of the Oi, Oa and Oe layers until stage 6 was 2.8 ± 0.4 cm while from stage 7 average thickness increased to 22.1 ± 3.0 cm.

Litter (Oi layer) C concentrations increased with time across the overall chronosequence ($P < 0.001$; $r = 0.594$), while N concentrations in litter decreased ($P = 0.006$; $r = -0.37$) and C: N ratios increased with time ($P < 0.001$; $r = 0.73$) (Fig. 2). Litter $\delta^{13}C$ values ranged between −33.1 and −28.4 ‰ and significantly decreased by *c.* 2 ‰ ($P < 0.001$; $r = -0.61$) across the chronosequence (Fig. 3a). $\delta^{15}N$ values in litter varied in a much wider range between −4.8 and 1.3 ‰ but we could not find an overall trend across the chronosequence, rather two declines in litter $\delta^{15}N$ values. The organic layer (Oe and Oa layer) was characterized by decreasing $\delta^{13}C$ values ($P = 0.024$; $r = -0.60$) with time (Fig. 3a). In mineral soil, we found an overall increase in C: N ratios ($P < 0.001$; $r = 0.75$) and in $\delta^{15}N$ values ($P < 0.001$; $r = 0.75$).

We found significant linear changes with time in element concentrations, C: N ratios and isotopic signatures in litter and mineral soil during the early (stages 0–2) and the late phase (stages 7–10), while the intermediate phase (stages 3–6) was lacking significant trends. Early ecosystem development was characterized by a strong increase in mineral soil C concentrations ($P < 0.001$; $r = 0.91$), a decrease in litter N concentrations ($P < 0.001$; $r = -0.81$) and an increase in mineral soil N concentrations ($P = 0.038$; $r = 0.54$), an increase in litter and mineral soil C: N ratios ($P < 0.001$; $r = 0.84$, 0.91) (Fig. 2) and decreasing $\delta^{13}C$ ($P = 0.016$; $r = -0.61$) and $\delta^{15}N$ values ($P < 0.001$; $r = -0.93$) (Fig. 3). During the late ecosystem development, we found similar trends in litter as compared to the early ecosystem development, i.e. a second decrease in litter N concentrations ($P = 0.006$; $r = -0.60$), an increase in litter C: N ratios ($P = 0.005$; $r = 0.60$) (Fig. 2) and decreasing $\delta^{13}C$ ($P = 0.004$; $r = -0.62$) and $\delta^{15}N$ values ($P = 0.003$; $r = -0.63$) (Fig. 3) with time. Stages 4 to 8 featured mean $\delta^{15}N$ values with −2.1 ± 0.2 ‰

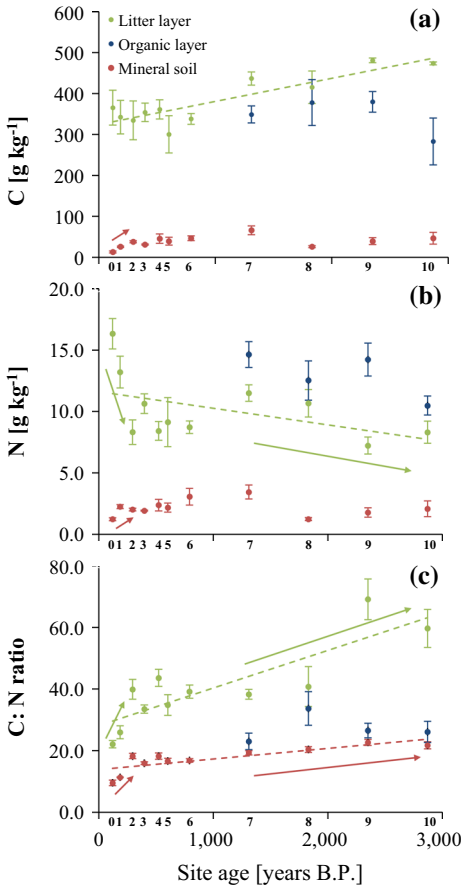

Fig. 2 Mean ± SE C (**a**) and N concentrations (g kg^{-1}) (**b**) and C:N ratios (**c**) in litter (Oi horizon), organic layers (Oe and Oa horizons) and mineral soil as functions of site age in years before present (B.P.). *Dotted lines* depict significant linear trends across the overall chronosequence, while arrows depict linear trends during the early (stages 0–2), the intermediate (stages 3–6) or the late (stages 7–10) phase of ecosystem development. *Numbers* at the *x* axis represent the dune stages referring to Table 1. *Error bars* are two SE and represent variation on one dune with $n = 5$

but wide ranges in litter $\delta^{15}N$ values, always with maximum values converging to the atmospheric signature (0 ‰). In addition, C: N ratios ($P = 0.011$; $r = 0.55$) and $\delta^{13}C$ values ($P = 0.003$; $r = 0.64$) increased in mineral soil during the late phase.

Vertical differences in $\delta^{13}C$ and $\delta^{15}N$ values and beta values with proceeding pedogenesis

We found a mean enrichment in ^{13}C of $\Delta^{13}C = 1.9 \pm 0.1$ ‰ and a three times greater enrichment in ^{15}N of $\Delta^{15}N = 6.0 \pm 0.3$ ‰ in profiles from litter to mineral soil. In 40 % of the profiles, mineral soil C concentrations and $\delta^{13}C$ values at 10 cm depth matched with the observed minimum C concentration and maximum $\delta^{13}C$ values. In the other profiles ($n = 32$), we found 2.5 ± 0.6 g kg^{-1} higher C concentrations and 0.2 ± 0.3 ‰ lower $\delta^{13}C$ values in the mineral soil at 10 cm depth, corresponding to 11.4 and 0.7 % variation, respectively. The variation was less pronounced for N concentrations. In 33 % of the profiles ($n = 18$), N concentrations were higher by 0.2 ± 0.0 g N kg^{-1} as compared to minimum N, while in 70 % of the profiles ($n = 38$) $\delta^{15}N$ values in the mineral soil at 10 cm depth deviated by 0.7 ± 0.1 ‰ from maximum $\delta^{15}N$ values corresponding to 15.4 and 21.9 % variation, respectively. In total, the vertical variation from a continuous C and N decrease and an isotopic enrichment of ^{13}C and ^{15}N was considered negligible.

Absolute values of linear regression slopes (=$beta_C$) between $\log_{10}$ (g C kg^{-1}) and according $\delta^{13}C$ values served to describe vertical isotopic patterns with mean $beta_C$ value of 1.2 ± 0.1. Linear regressions were significant in 90 % of the profiles ($n = 51$). Non-significant regressions ($P > 0.05$) were observed at sites 0B, 5B, 6D, 7E and 8D (Fig S1). To omit bias, $beta_C$ values of these regressions were included in further analyses. Mean R^2 was 0.67 ± 0.0. In 95 % of the profiles ($n = 52$) $beta_N$ values resulted from significant linear regressions between $\log_{10}$ (10^{-1} g N kg^{-1}) and according $\delta^{15}N$. Non-significant regressions ($P \geq 0.05$) were observed at sites 5B, 6A and 9B (Fig S2). Mean $beta_N$ value was 5.0 ± 0.3 with $R^2 = 0.77 \pm 0.0$. Residuals were normally distributed in either case both for regressions of C and N. Sites with a distinguishable accumulated organic layer (soil age ≥ 1300 years B.P.) featured a lower proportion of explained variation of 20 %. Thus, R^2 at sites with an accumulated organic layer (stages 0–6: $R^2 = 0.75 \pm 0.0$; stages 7–10: $R^2 = 0.54 \pm 0.0$) were significantly lower for relations between $\log_{10}$ (g C kg^{-1}) and $\delta^{13}C$ values ($P = 0.008$) and for relations between $\log_{10}$ (10^{-1} g N kg^{-1}) and $\delta^{15}N$ values (stages 0–6: $R^2 = 0.83 \pm 0.0$; stages 7–10: $R^2 = 0.54 \pm 0.0$) ($P = 0.015$).

$\Delta^{13}C$ ($P = 0.001$; $r = 0.49$) and $\Delta^{15}N$ ($P < 0.001$; $r = 0.77$) linearly increased with time across the overall chronosequence. In contrast, $beta_C$ and $beta_N$ values did not show significant linear trends (Fig. 3c, d). For every one per mill increase in ^{13}C, OM

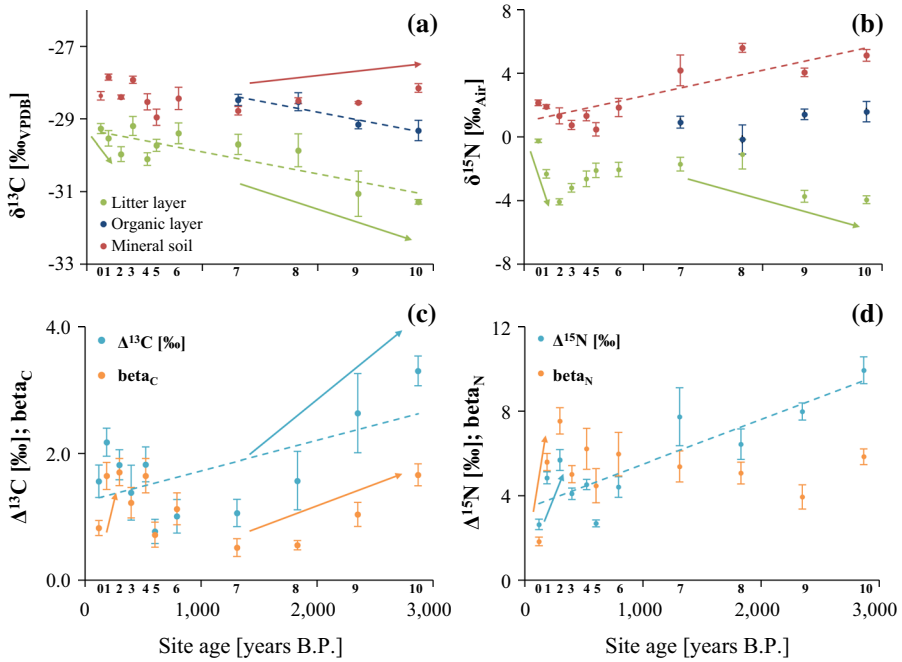

Fig. 3 Mean ± SE $\delta^{13}C$ (‰$_{VPDB}$) (**a**) and $\delta^{15}N$ (‰$_{Air}$) values (**b**) in the litter layer (Oi horizon), the organic layers (Oe and Oa horizons) and in the mineral soil. Maximum isotopic difference from litter to mineral soil in ^{13}C (**c**) and ^{15}N (**d**) is given as $\Delta^{13}C$ and $\Delta^{15}N$. Beta$_C$ (**c**) and beta$_N$ (**d**) values represent absolute values of regression slopes between $\log_{10}x$ element concentrations and isotopic signatures. All values as functions of site age in years before present (B.P.). *Dotted lines* depict significant linear trends across the overall chronosequence, while arrows depict linear trends during the early (stages 0–2), the intermediate (stages 3–6) or the late (stages 7–10) phase of ecosystem development. *Numbers* at the *x* axis represent the dune stages referred to Table 1. *Error bars* are two standard errors and represent variation on one dune with $n = 5$

increased by 3.1 ± 0.2 ‰ in ^{15}N. Beta$_C$ and $\Delta^{13}C$ values were significantly related ($P < 0.001$; $r = 0.65$), similarly to beta$_N$ and $\Delta^{15}N$ values ($P = 0.007$; $r = 0.36$). In addition, $\Delta^{13}C$ and $\Delta^{15}N$ were significantly related ($P < 0.001$; $r = 0.52$), similarly to beta$_C$ and beta$_N$ ($P < 0.001$; $r = 0.47$). During the early phase, we found increasing trends of $\Delta^{15}N$ values ($P < 0.001$; $r = 0.81$), beta$_C$ values ($P = 0.018$; $r = 0.60$) and beta$_N$ values ($P < 0.001$; $r = 0.89$). Slight but not significantly higher beta$_N$ values (5.0 ± 0.4) compared to $\Delta^{15}N$ (4.1 ± 0.2 ‰) during the early and the intermediate phase disclose the deviation of vertical ^{15}N enrichment with depth. Those effects were obscured by stronger impacts of litter and organic layers on the regression slopes at the later stages. We found no linear trends of isotopic differences and beta values during the intermediate phase. However, $\Delta^{13}C$ was lowest in this phase of the chronosequence (1.2 ± 0.2 ‰) as compared to the early (1.9 ± 0.1 ‰) and the late phase (2.1 ± 0.3 ‰) ($P < 0.025$). The late phase featured increasing $\Delta^{13}C$ values ($P < 0.001$; $r = 0.72$) and increasing beta$_C$ values ($P < 0.001$; $r = 0.79$). There were no linear trends of $\Delta^{15}N$ values in the late phase, but these values were with mean $\Delta^{15}N$ of 8.0 ± 0.5 ‰ significantly higher at the late phase as compared to the early (4.4 ± 0.4 ‰) and the intermediate (3.9 ± 0.2 ‰) phase ($P < 0.001$).

Discussion

$\delta^{13}C$ and $\delta^{15}N$ values in litter with proceeding pedogenesis

As a result of a possible morphological adaption to deceasing nutrient availability with time, we hypothesized that litter $\delta^{13}C$ values increase with proceeding ecosystem development and pedogenesis. However, we observed a decrease in litter $\delta^{13}C$ values with site age (Fig. 3a) which was contrary to findings across boreal chronosequences (Clemmensen et al. 2013;

Hyodo et al. 2013; Hyodo and Wardle 2009) and therefore falsifies our first hypothesis. The following parameters might be involved in explaining the decreased $\delta^{13}C$ values of litter (i) soil respiration, (ii) irradiance, (iii) nutrient limitation. At Haast, there is an increasing abundance of moss, understory species and seedlings with site age (Turner et al. 2012b) which utilize a greater proportion of ^{13}C depleted CO_2 respired from soil (Hyodo and Wardle 2009) and are exposed to a lower irradiance which would both result in lower $\delta^{13}C$ values in litter (Fotelli et al. 2003; Hyodo and Wardle 2009) and could therefore induce a decrease in litter $\delta^{13}C$ with time. On the other hand, root respired CO_2 of woody species or of species associated with mycorrhiza was found to be ^{13}C enriched (Ghashghaie and Badeck 2014). Therefore, respiration impacts on plants remain indistinct and cannot clearly be related to changed litter $\delta^{13}C$ values. Due to the close distance of the dunes (<5 km), we exclude spatial variations in humidity, since the humid climate would not cause differences on stomatal conductance.

Nutrient limitation provides another explanation for lower litter $\delta^{13}C$ values as it is shown by decreasing N concentrations of litter and increasing C: N ratios across the chronosequence (Fig. 2). Nutrient limitation promotes plant stress which could either force plants to adapt morphologically, resulting in increased $\delta^{13}C$ values as it was found in boreal systems (Hyodo et al. 2013; Hyodo and Wardle 2009), or nutrient limitation can induce increased stomatal conductivity and therefore a higher photosynthetic fractionation (Cernusak et al. 2013; Farquhar et al. 1989; Peltzer et al. 2010). Although P is typically thought to limit primary production on older surfaces (Vitousek and Farrington 1997; Walker and Syers 1976), we observed decreasing litter N concentrations and decreasing $\delta^{13}C$ values, similar to results from other studies (Guehl et al. 1995; Vitousek et al. 1990). Thus, it is possible that nutrient limitation may have driven the depletion of ^{13}C in litter. In contrast to findings across chronosequences in boreal ecosystems, decreasing $\delta^{13}C$ values of litter suggest a physiological response rather than a morphological adaption to changes in nutrient dynamics in this temperate rainforest system.

Our second hypothesis assuming that litter $\delta^{15}N$ values are close to the atmospheric signature due to the contribution of N via biological N_2 fixation across the overall Haast chronosequence cannot be fully verified. The $\delta^{15}N$ signature of litter suggests biological N_2 fixation occurring in the early stages of ecosystem development with a decline at *c.* 300 years and a subsequent increase of N_2 fixation again at stages 4–8, but at this time rather related to free-living than symbiotic pathways of N_2 fixation. Immediately after dune formation, we found $\delta^{15}N$ values in litter of -0.3 ± 0.1 ‰ (Fig. 3b). Atmospheric N_2 fixing legumes, e.g. the visibly dominant species broom (*Cytisus scoparius*) that colonized the beachfront dune likely converged litter $\delta^{15}N$ values to the atmospheric value and raised C and N concentrations in mineral soil in the following development (Fig. 2b). According to the visible abundance of legumes and litter $\delta^{15}N$ values close to zero, biological N_2 fixation appears to be important during ecosystem establishment at Haast which supports the outstanding role in N supply by biological N_2 fixation during early succession (Menge and Hedin 2009; Vitousek et al. 2013).

The subsequent decrease of litter $\delta^{15}N$ values within the first *c.* 300 years of ecosystem development (Fig. 3b) suggests a reduced N_2 fixation rate. Reduced N_2 fixation during the early phase might be related to the growing overstory vegetation, since N_2 fixers were found to be shade-intolerant (Vitousek et al. 2013) or to species replacement as it was found for a symbiotic N_2 fixing plant at the Franz Josef chronosequence (Menge and Hedin 2009). While it is accepted that a higher N availability reduces N_2 fixation (DeLuca et al. 2008; Menge and Hedin 2009), which could additionally well explain a reduction of N_2 fixation, we found that N concentrations of litter decreased in the early phase, that rather argues for a reduced N availability. This decreased N availability during the early phase at Haast is linked with a decrease in litter $\delta^{15}N$ values and therefore in line with literature data where positive relations between N availability and litter $\delta^{15}N$ values were widely presented (Craine et al. 2015). In addition, different N_2 fixation strategies (Menge et al. 2015; Reed et al. 2011) may exist at Haast and could be decoupled from N availability. However, reduced N_2 fixation combined with reduced N availability raises the importance of other N nutrition forms to maintain N acquisition. Utilization of nitrate (NO_3^-) (Templer et al. 2007) or N supply by mycorrhizal fungi (Hobbie et al. 1999; Hyodo et al. 2013) would both result in distinct depletion of ^{15}N in litter. On the other hand,

readily available mineral forms of N were found to induce a reduction of biological N_2 fixation (Reed et al. 2011) calling for further studies on function, species composition and possible switch off of N_2 fixers to clarify our findings.

Between stages 4–8 (*c.* 523 to *c.* 1830 years), $\delta^{15}N$ values of litter converging closer to zero suggest N_2 fixation, while lower $\delta^{15}N$ values of litter rather argue for a supply with other N forms, e.g. through fungi or mycorrhiza (Hobbie and Högberg 2012). Dinitrogen fixation during the intermediate stages could confirm the activity of diazotrophic N_2 fixers, since abundances of N_2 fixing bacterial rRNA genes were observed at Haast (Jangid et al. 2013). In addition, the role of N_2 fixing bryophytes and lichens colonizing the more diverse and tall habitats during the intermediate stages could have been increased. Menge and Hedin (2009) proposed a possible decoupling of N_2 fixation and N availability in soil, with these species possibly serving as a positive feedback to ecosystem N availability. Again, full documentation of N_2 fixing species composition might clarify the functioning of biological N_2 fixation at Haast. However, we assume that the intermediate phase featured mixed impacts of atmospheric N_2 fixation, i.e. symbiotic and free living N_2 fixation and supply with other recycled N forms, which might parallel the supposed heterogeneity associated with patches (Pickett and White 1985).

During the late phase (stages 7–10), we found a decline in litter $\delta^{15}N$ values (Fig. 3b) together with decreasing litter N concentrations and increasing C: N ratios (Fig. 2), similarly to the early phase. In the same manner, greater N availability as reduction of N_2 fixation could be excluded. Increasing mycorrhizal abundance with supply of ^{15}N depleted N, ^{15}N depleted N provided by litter decomposition (Menge et al. 2011) or a potential decrease of N_2 fixation under increasing P limitation (Vitousek and Howarth 1991) might serve as alternative explanations for decreasing $\delta^{15}N$ values of litter.

In summary, $\delta^{15}N$ values of litter converged to the atmospheric isotopic signature in the early succession and in the intermediate stages. However, under several conditions, e.g. changes in species composition, structural changes of the canopy or as a result of increasing P limitation, N_2 fixation seems to be replaced by other N nutrition forms and appeared to be not constantly dominant across the Haast chronosequence.

Vertical patterns of $\delta^{13}C$ values with proceeding pedogenesis

Thirdly, we hypothesized a continuous decrease in decomposition with time. However, $beta_C$ values as approximation of decomposition (Acton et al. 2013; Brunn et al. 2014; Diochon and Kellman 2008; Garten 2006; Guillaume et al. 2015; Marty et al. 2015) increased during early ecosystem development and at old sites, while they were lowest at the intermediate stages (1500 years) which falsifies our third hypothesis. Vertical $\delta^{13}C$ patterns described by $beta_C$ values (1.2 ± 0.1) and $\Delta^{13}C$ (1.9 ± 0.1 ‰) were at the lower end of data reported in the literature (Brunn et al. 2014; Garten 2006; Guillaume et al. 2015; Powers and Schlesinger 2002). This was possibly affected by the coarse soil texture at Haast that has been shown to influence isotope fractionation on mineral soil $\delta^{13}C$ values (Bird et al. 2003). Low vertical enrichment in ^{13}C might be exacerbated with root removal during our sample preparation. In systems where fungi are abundant, root removal could increase the amount of fungal remains (Hobbie and Ouimette 2009). Since fungi are ^{13}C depleted (Kohl et al. 2015) their contribution could lower $\delta^{13}C$ values in mineral soil samples and therefore the isotopic difference between litter and mineral soil OM. Impacts of a continuous decrease of atmospheric $\delta^{13}CO_2$ by 1.5 ‰ during the last two centuries (Francey et al. 1999; Keeling et al. 2005) might explain the observed average vertical change in $\delta^{13}C$. However, this Suess effect would result in $\Delta^{13}C$ values distinctly lower than 1.5 ‰ at the youngest site (<120 years) that contained no C before its formation. In addition, the Suess effect lacks in explaining variations in $\Delta^{13}C$ between dune stages >300 years, i.e. the atmospheric change as single driver of $\delta^{13}C$ depth profiles would result in more constant $\Delta^{13}C$ values. Together with findings from other studies (Acton et al. 2013; Guillaume et al. 2015), we infer that the Suess effect alone is not able to fully explain the vertical enrichment of ^{13}C in OM in soil profiles.

Increasing $beta_C$ values during the early phase of ecosystem development (Fig. 3c) suggest enhanced decomposition, probably stimulated through plant communities containing low abundances of woody species (Turner et al. 2012b). At stage 7 and 8, we observed lowest $beta_C$ values (Fig. 3c; Table S2). First generation trees collapsed after stage 6 and a

distinguishable organic layer started to accumulate from stage 7 on (Table 1). Fungi preferably colonize the organic horizon below the fresh litter layer (Lindahl et al. 2007) and the accumulated organic layer could therefore promote fungal colonization. Fungi and mycorrhiza are supposed to reduce decomposition rates (Clemmensen et al. 2015; Gadgil and Gadgil 1971; Langley and Hungate 2003) and could lower $beta_C$ values. Low $beta_C$ values were associated with relatively low $\delta^{13}C$ values in mineral soil (Table S1; Fig. 3a) probably governed by decreased microbial cycling and therefore a lower accumulation of ^{13}C enriched microbial products. In addition, Kramer et al. (2003) observed no vertical trends in $\delta^{13}C$ if OM is recycled from the structurally and chemically altered organic layer.

While we can mechanistically explain a possible reduction in decomposition rates from early to the intermediate stages, we lack an explanation for the increase of $beta_C$ values at the later stages. Stimulated decomposition probably owing to a reduced canopy closure after the collapse of first generation trees likely lowered organic layer thickness at stage 10 as compared to stages 8 and 9 (Table 1). However, increasing decomposition is against our third hypothesis that decomposition declines constantly across the chronosequence according to the retrogressive model (Peltzer et al. 2010). And increasing decomposition contradicts the reduced N concentrations in litter attributed to a lower N availability (Fig. 2).This implies that the later stages do not belong to the retrogressive phase and could be better described as transition time characterized by an elevated decomposition, e.g. related to canopy opening. Higher decomposition results in elevated ^{13}C enriched decomposition products (Billings and Richter 2006) and together with a shift to slightly finer soil texture (Turner et al. 2012a) that facilitate a better sorption capacity of enriched microbial products (Bird et al. 2003), higher decomposition results in increased $\delta^{13}C$ values in mineral soil at the late stages. Alternatively, $beta_C$ values could be insufficient to describe decomposition at sites with an accumulated organic layer. Including the organic layer (Oe and Oa layer) with high C concentrations but strong ^{13}C enrichment (Fig. 1) into linear regressions between $\log_{10}$ (g C kg^{-1}) and $\delta^{13}C$ values results in less steep regression lines, visible in diverging $\Delta^{13}C$ and $beta_C$ values as soils age (Fig. 3c). Lower $\delta^{13}C$ values of litter at later stages might suggest that litter layers control the vertical isotopic gradients. In dependence of an decomposition continuum from less decomposed litter to more decomposed OM in the mineral soil (Melillo et al. 1989), $\delta^{13}C$ values of litter form part of the vertical patterns in isotopic enrichment and should therefore not control vertical isotopic gradients. This decomposition continuum can be underpinned by manganese (Mn) concentrations in litter (unpublished data). Manganese concentrations in litter were found to be positively related to litter decomposition (Berg et al. 2007; Keiluweit et al. 2015). Significant linear relations between litter Mn concentrations and $beta_C$ values at Haast ($r = 0.41$; $P = 0.002$) suggest the applicability for beta values as an indicator of decomposition. However, the falsification of our third hypothesis merits further detailed studies of the quality of $beta_C$ values and the interplay between the accumulation of an organic layer, decomposition rates, and the translocation of organic compounds to deeper spodic horizons (not considered in our study) at older sites.

Vertical patterns in $\delta^{15}N$ values with proceeding pedogenesis

Our fourth hypothesis was that differences between $\delta^{15}N$ values of litter and mineral soil OM increase with time resulting in increasing $beta_N$ values. Average $beta_N$ (5.0 ± 0.3) and $\Delta^{15}N$ values (6.0 ± 0.4 ‰) were in line with literature data reviewed by Hobbie and Ouimette (2009). The wide range of observed data ($beta_N$ between 1.3 and 9.3; $\Delta^{15}N$ between 1.7 and 13.0 ‰) suggests a diversity of dominant fractionation processes across the chronosequence, e.g. mineralization in soil (Dijkstra et al. 2006) or changes in mycorrhizal fungal association (Hobbie and Ouimette 2009). $\delta^{15}N$ values in soil as one component of the difference between litter and soil increased continuously with proceeding dune age (Fig. 3). This might be caused by "stripping": During mineralization, the dynamic exchange of microbially derived hydrophilic and plant derived hydrophobic OM and subsequent continuous stripping throughout the soil profile (Kusliene et al. 2015). This concept relies on the most abundant forms of transported N, being dissolved organic N (DON) combined with NH_4^+ in unpolluted areas (Perakis and Hedin 2002). Since NH_4^+ and microbial biomass are enriched in ^{15}N (Dijkstra et al.

2006; Templer et al. 2007), the mixing of microbial versus plant derived OM result in stripping of charged OM that is retained in soil, whereas non-charged compounds will be transported downwards. This stripping is controlled by sorption sites and thus, soil texture. In our chronosequence, the shift to soils with slightly finer textures (Turner et al. 2012a) together with increased aggregate formation and stabilization by fungal hyphae (Rillig et al. 2015) might feature greater sorption capacity through organo-mineral-complexes with increased site age and therefore probably amplify the $\delta^{15}N$ increase in mineral soil with time.

If combined with litter $\delta^{15}N$ values, during early succession, $\Delta^{15}N$ and $beta_N$ values strongly increased, supporting the assumption of fungal colonization in this time owing to fractionation against ^{15}N and thus, ^{15}N-depleted N transferred to plants. As a result, low $\delta^{15}N$ values of litter further increase the difference between litter and mineral soil and thus, also vertical patterns. In addition, microbial recycling of OM originating from the structurally and compositionally altered organic layer rather than from fresh litter (Kramer et al. 2003) or greater proportions of ^{15}N-enriched fungal remains (Hobbie and Högberg 2012) could explain elevated $\delta^{15}N$ values in mineral soil from stage 7 on. In line, AM that were host specific for kamahi (*Weinmannia racemosa)* at the nearby Franz-Josef chronosequence (Martinez-Garcia et al. 2015) could also be dominant at Haast, where kamahi regenerates in tree-fall gaps (Turner et al. 2012b). However, mean isotopic enrichment during the late phase ($\Delta^{15}N$) of 8.0 ± 0.5 ‰ was greater than gradients observed in AM-dominated systems (Hobbie and Ouimette 2009). At stage 10, we observed an isotopic enrichment ($\Delta^{15}N$) of 9.9 ± 0.6 ‰ that is in line with ^{15}N enrichment found in EM-dominated systems (Hobbie and Ouimette 2009). Thus, the increasing abundance of ectomycorrhizal Silver beech (*Nothofagus menziesii*) (Turner et al. 2012b) might also explain elevated mineral soil $\delta^{15}N$ values at the late stages.

The contribution of denitrification to the enrichment of ^{15}N in soils, as it has been widely observed (Craine et al. 2015; Houlton and Bai 2009; Houlton et al. 2006) was found to not occur or being not expressed at the nearby Franz Josef chronosequence (Menge et al. 2011). Although waterlogging was excluded at Haast (Turner et al. 2012a), we are unable to exclude impacts on gaseous N losses on isotopic signatures in soil profiles that may also account for greater $\delta^{15}N$ values in mineral soil and therefore to more distinct depth profiles. However, a possible increase of $\delta^{15}N$ values in mineral soil induced by denitrification contradicts the decrease of $\delta^{15}N$ values of litter during the late phase (Fig. 3).

Analogous to relations between $beta_C$ and $\Delta^{13}C$, we found $beta_N$ and $\Delta^{15}N$ values diverging as soils aged (Fig. 3d). Similarly, the accumulated organic layer seems to contribute to this trend, i.e. including the organic layer, containing even higher N concentrations but being strongly ^{15}N enriched compared to the litter layer (Fig. 1), into linear regressions between $\log_{10}$ (10^{-1} g N kg^{-1}) and $\delta^{15}N$ values results in less steep regression lines. Our fourth hypothesis that $beta_N$ values increase with site age cannot fully be verified, since only $\Delta^{15}N$ increased across the chronosequence but not $beta_N$ values, probably indicating that despite effects of mycorrhizal fractionation other processes affect $\delta^{15}N$ depth profiles during ecosystem development and pedogenesis.

Conclusion

The findings of this study provided new information on C and N dynamics occurring during *c.* 2870 years of soil and ecosystem development across the temperate rainforest Haast dune chronosequence. In contrast to findings across boreal chronosequences, we found $\delta^{13}C$ values in litter decreasing with time, probably indicating a physiological rather than a morphological adaption to changes in nutrient dynamics. Litter $\delta^{15}N$ values suggested N_2 fixation that might be attributable to the activity of diazotrophs identified at Haast. However, other N nutrition forms, e.g. utilization of NO_3^- or N supply by mycorrhizal fungi likely contributed to two declines in litter $\delta^{15}N$ values, one in the early phase (between 120 and 296 *yrs*) and a second decline in the late phase (between 1300 and 2870 *yrs*). Against our hypothesis, decomposition (approximated with linear regression slopes between $\log_{10}$ (g C kg^{-1}) and $\delta^{13}C$ values) did not constantly decrease with time. Instead, we found an increase of decomposition at the beginning of ecosystem development and a second increase in the late phase. Lowest decomposition during the intermediate phase matched with the accumulation of the organic layer. Increasing

decomposition during the late phase might indicate dynamics linked with canopy opening after the collapse of first generation trees. While we have indications that $\delta^{15}N$ depth profiles are related to mycorrhizal fractionation as it is reported in the literature, additional processes might affect $\delta^{15}N$ depth profiles during ecosystem development. Interestingly, we found relations between $beta_C$ and $beta_N$ values, similarly to $\Delta^{13}C$ and $\Delta^{15}N$, suggesting that there might be shared processes shaping $\delta^{13}C$ and $\delta^{15}N$ depth profiles, e.g. microbial cycling, transport or sorption. However, further manipulative experiments and measurements of different N_2 fixation pathways are needed to underpin the assumed mechanisms and causal connections, particularly the role of mycorrhizal associations and forms of N_2 fixation, vertical transport and sorption processes and the functioning of the organic layer.

Acknowledgments We thank G. Guggenberger, L. Sauheitl and S. Bokeloh (Leibniz University Hanover, Germany) for providing isotopic analysis, U. Bange, M. Kraft and A. Bell (University of Koblenz-Landau, Germany) for laboratory assistance, A. Torky and N. Franks (Lincoln University, New Zealand) for organizing the sample transport and W. Wilcke (Karlsruhe Institute of Technology, Germany) and F. Brunn (University of Mainz, Germany) for facilitating this work. We gratefully acknowledge research funding by the German Academic Exchange Service (DAAD Grant D/12/45516).

References

Acton P, Fox J, Campbell E, Rowe H, Wilkinson M (2013) Carbon isotopes for estimating soil decomposition and physical mixing in well-drained forest soils. J Geophys Res Biogeosci 118(4):1532–1545

Andrews M, James EK, Sprent JI, Boddey RM, Gross E, dos Reis FB (2011) Nitrogen fixation in legumes and actinorhizal plants in natural ecosystems: values obtained using N-15 natural abundance. Plant Ecol Divers 4(2–3):131–140

Berg B, Steffen KT, McClaugherty C (2007) Litter decomposition rate is dependent on litter Mn concentrations. Biogeochemistry 82(1):29–39

Billings SA, Richter DD (2006) Changes in stable isotopic signatures of soil nitrogen and carbon during 40 years of forest development. Oecologia 148(2):325–333

Bird M, Kracht O, Derrien D, Zhou Y (2003) The effect of soil texture and roots on the stable carbon isotope composition of soil organic carbon. Aust J Soil Res 41(1):77–94

Brunn M, Spielvogel S, Sauer T, Oelmann Y (2014) Temperature and precipitation effects on delta C-13 depth profiles in SOM under temperate beech forests. Geoderma 235:146–153

Cernusak LA, Ubierna N, Winter K, Holtum JAM, Marshall JD, Farquhar GD (2013) Environmental and physiological determinants of carbon isotope discrimination in terrestrial plants. New Phytol 200(4):950–965

Clemmensen KE, Bahr A, Ovaskainen O, Dahlberg A, Ekblad A, Wallander H, Stenlid J, Finlay RD, Wardle DA, Lindahl BD (2013) Roots and associated fungi drive long-term carbon sequestration in boreal forest. Science 339(6127):1615–1618

Clemmensen KE, Finlay RD, Dahlberg A, Stenlid J, Wardle DA, Lindahl BD (2015) Carbon sequestration is related to mycorrhizal fungal community shifts during long-term succession in boreal forests. New Phytol 205(4):1525–1536

Craine JM, Brookshire ENJ, Cramer MD, Hasselquist NJ, Koba K, Marin-Spiotta E, Wang LX (2015) Ecological interpretations of nitrogen isotope ratios of terrestrial plants and soils. Plant Soil 396(1–2):1–26

DeLuca TH, Zackrisson O, Gundale MJ, Nilsson MC (2008) Ecosystem feedbacks and nitrogen fixation in boreal forests. Science 320(5880):1181

Dickie IA, Martinez-Garcia LB, Koele N, Grelet GA, Tylianakis JM, Peltzer DA, Richardson SJ (2013) Mycorrhizas and mycorrhizal fungal communities throughout ecosystem development. Plant Soil 367(1–2):11–39

Dijkstra P, Ishizu A, Doucett R, Hart SC, Schwartz E, Menyailo OV, Hungate BA (2006) C-13 and N-15 natural abundance of the soil microbial biomass. Soil Biol Biochem 38(11):3257–3266

Diochon A, Kellman L (2008) Natural abundance measurements of (13)C indicate increased deep soil carbon mineralization after forest disturbance. Geophys Res Lett 35(14):1–5

Eger A, Almond PC, Condron LM (2011) Pedogenesis, soil mass balance, phosphorus dynamics and vegetation communities across a Holocene soil chronosequence in a superhumid climate, South Westland, New Zealand. Geoderma 163(3–4):185–196

Farquhar GD, Ehleringer JR, Hubick KT (1989) Carbon isotope discrimination and photosynthesis. Annu Rev Plant Physiol Plant Mol Biol 40:503–537

Fotelli MN, Rennenberg H, Holst T, Mayer H, Gessler A (2003) Carbon isotope composition of various tissues of beech (*Fagus sylvatica*) regeneration is indicative of recent environmental conditions within the forest understorey. New Phytol 159(1):229–244

Francey RJ, Allison CE, Etheridge DM, Trudinger CM, Enting IG, Leuenberger M, Langenfelds RL, Michel E, Steele LP (1999) A 1000-year high precision record of delta C-13 in atmospheric CO2. Tellus Ser B Chem Phys Meteorol 51(2):170–193

Gadgil RL, Gadgil PD (1971) Mycorrhiza and litter decomposition. Nature 233(5315):133

Galloway JN, Dentener FJ, Capone DG, Boyer EW, Howarth RW, Seitzinger SP, Asner GP, Cleveland CC, Green PA, Holland EA, Karl DM, Michaels AF, Porter JH, Townsend AR, Vorosmarty CJ (2004) Nitrogen cycles: past, present, and future. Biogeochemistry 70(2):153–226

Garten CT (2006) Relationships among forest soil C isotopic composition, partitioning, and turnover times. Can J For Res 36(9):2157–2167

Garten CT, Iversen CM, Norby RJ (2011) Litterfall N-15 abundance indicates declining soil nitrogen availability in a free-air CO2 enrichment experiment. Ecology 92(1):133–139

Ghashghaie J, Badeck FW (2014) Opposite carbon isotope discrimination during dark respiration in leaves versus roots—a review. New Phytol 201(3):751–769

Guehl JM, Fort C, Ferhi A (1995) Differential response of leaf conductance, carbon isotope discrimination and water-use efficiency to nitrogen deficiency in maritime pine and pedunculate oak plants. New Phytol 131(2):149–157

Guillaume T, Damris M, Kuzyakov Y (2015) Losses of soil carbon by converting tropical forest to plantations: erosion and decomposition estimated by delta C-13. Glob Change Biol 21(9):3548–3560

Hobbie EA, Högberg P (2012) Nitrogen isotopes link mycorrhizal fungi and plants to nitrogen dynamics. New Phytol 196(2):367–382

Hobbie EA, Ouimette AP (2009) Controls of nitrogen isotope patterns in soil profiles. Biogeochemistry 95(2–3):355–371

Hobbie EA, Macko SA, Shugart HH (1999) Insights into nitrogen and carbon dynamics of ectomycorrhizal and saprotrophic fungi from isotopic evidence. Oecologia 118(3):353–360

Högberg P (1997) Tansley review No 95 - N-15 natural abundance in soil-plant systems. New Phytol 137(2):179–203

Houlton BZ, Bai E (2009) Imprint of denitrifying bacteria on the global terrestrial biosphere. Proc Natl Acad Sci USA 106(51):21713–21716

Houlton BZ, Sigman DM, Hedin LO (2006) Isotopic evidence for large gaseous nitrogen losses from tropical rainforests. Proc Natl Acad Sci USA 103(23):8745–8750

Hyodo F, Wardle DA (2009) Effect of ecosystem retrogression on stable nitrogen and carbon isotopes of plants, soils and consumer organisms in boreal forest islands. Rapid Commun Mass Spectrom 23(13):1892–1898

Hyodo F, Kusaka S, Wardle DA, Nilsson MC (2013) Changes in stable nitrogen and carbon isotope ratios of plants and soil across a boreal forest fire chronosequence. Plant Soil 367(1–2):111–119

Jangid K, Whitman WB, Condron LM, Turner BL, Williams MA (2013) Progressive and retrogressive ecosystem development coincide with soil bacterial community change in a dune system under lowland temperate rainforest in New Zealand. Plant Soil 367(1–2):235–247

Jones AR, Sanderman J, Allen D, Dalal R, Schmidt S (2015) Subtropical giant podzol chronosequence reveals that soil carbon stabilisation is not governed by litter quality. Biogeochemistry 124(1–3):205–217

Keeling CD, Piper SC, Bacastow RB, Wahlen M, Whorf TP, Heimann M, Meijer HA (2005) Atmospheric CO2 and (CO2)-C-13 exchange with the terrestrial biosphere and oceans from 1978 to 2000: observations and carbon cycle implications. In: Ehleringer JR, Cerling TE, Dearing MD (eds) Ecological studies: analysis and synthesis. Springer, New York, pp 83–113

Keiluweit M, Nico P, Harmon ME, Mao JD, Pett-Ridge J, Kleber M (2015) Long-term litter decomposition controlled by manganese redox cycling. Proc Natl Acad Sci USA 112(38):E5253–E5260

Kohl L, Laganiere J, Edwards KA, Billings SA, Morrill PL, Van Biesen G, Ziegler SE (2015) Distinct fungal and bacterial delta C-13 signatures as potential drivers of increasing delta C-13 of soil organic matter with depth. Biogeochemistry 124(1–3):13–26

Körner C, Diemer M (1987) In situ photosynthetic responses to light, temperature and carbon dioxide in herbaceous plants from low and high altitude. Funct Ecol 1(3):179–194

Kramer MG, Sollins P, Sletten RS, Swart PK (2003) N isotope fractionation and measures of organic matter alteration during decomposition. Ecology 84(8):2021–2025

Krull ES, Bestland EA, Gates WP (2002) Soil organic matter decomposition and turnover in a tropical ultisol: evidence from delta C-13, delta N-15 and geochemistry. Radiocarbon 44(1):93–112

Kusliene G, Eriksen J, Rasmussen J (2015) Leaching of dissolved organic and inorganic nitrogen from legume-based grasslands. Biol Fertil Soils 51(2):217–230

Langley JA, Hungate BA (2003) Mycorrhizal controls on belowground litter quality. Ecology 84(9):2302–2312

Lerch TZ, Nunan N, Dignac MF, Chenu C, Mariotti A (2011) Variations in microbial isotopic fractionation during soil organic matter decomposition. Biogeochemistry 106(1):5–21

Lindahl BD, Ihrmark K, Boberg J, Trumbore SE, Hogberg P, Stenlid J, Finlay RD (2007) Spatial separation of litter decomposition and mycorrhizal nitrogen uptake in a boreal forest. New Phytol 173(3):611–620

Martinelli LA, Piccolo MC, Townsend AR, Vitousek PM, Cuevas E, McDowell W, Robertson GP, Santos OC, Treseder K (1999) Nitrogen stable isotopic composition of leaves and soil: tropical versus temperate forests. Biogeochemistry 46(1–3):45–65

Martinez-Garcia LB, Richardson SJ, Tylianakis JM, Peltzer DA, Dickie IA (2015) Host identity is a dominant driver of mycorrhizal fungal community composition during ecosystem development. New Phytol 205(4):1565–1576

Marty C, Houle D, Gagnon C (2015) Effect of the relative abundance of conifers versus hardwoods on soil delta C-13 enrichment with soil depth in Eastern Canadian forests. Ecosystems 18(4):629–642

Melillo JM, Aber JD, Linkins AE, Ricca A, Fry B, Nadelhoffer KJ (1989) Carbon and nitrogen dynamics along the decay continuum—plant litter to soil organic-matter. Plant Soil 115(2):189–198

Menge DNL, Hedin LO (2009) Nitrogen fixation in different biogeochemical niches along a 120 000-year chronosequence in New Zealand. Ecology 90(8):2190–2201

Menge DNL, Baisden WT, Richardson SJ, Peltzer DA, Barbour MM (2011) Declining foliar and litter delta 15N diverge from soil, epiphyte and input delta 15N along a 120 000 yr temperate rainforest chronosequence. New Phytol 190(4):941–952

Menge DNL, Wolf AA, Funk JL (2015) Diversity of nitrogen fixation strategies in Mediterranean legumes. Nat Plants 1(6):1–5

Nadelhoffer KF, Fry B (1988) Controls on natural N-15 and C-13 abundances in forest soil organic-matter. Soil Sci Soc Am J 52(6):1633–1640

Peltzer DA, Wardle DA, Allison VJ, Baisden WT, Bardgett RD, Chadwick OA, Condron LM, Parfitt RL, Porder S, Richardson SJ, Turner BL, Vitousek PM, Walker J, Walker LR (2010) Understanding ecosystem retrogression. Ecol Monogr 80(4):509–529

Perakis SS, Hedin LO (2002) Nitrogen loss from unpolluted South American forests mainly via dissolved organic compounds. Nature 415(6870):416–419

Pickett STA, White PS (1985) The ecology of natural disturbance and patch dynamics. Academic Press, Orlando, p 472

Powers JS, Schlesinger WH (2002) Geographic and vertical patterns of stable carbon isotopes in tropical rain forest soils of Costa Rica. Geoderma 109(1–2):141–160

Reed SC, Cleveland CC, Townsend AR (2011) Functional ecology of free-living nitrogen fixation: a contemporary perspective. In: Futuyma DJ, Shaffer HB, Simberloff D (eds) Annual review of ecology, evolution, and systematics, vol 42. Annual Reviews, Palo Alto, pp 489–512

Rillig MC, Aguilar-Trigueros CA, Bergmann J, Verbruggen E, Veresoglou SD, Lehmann A (2015) Plant root and mycorrhizal fungal traits for understanding soil aggregation. New Phytol 205(4):1385–1388

Savin NE, White KJ (1977) Durbin–Watson test for serial—correlation with extreme sample sizes or many regressors. Econometrica 45(8):1989–1996

Schmidt MWI, Torn MS, Abiven S, Dittmar T, Guggenberger G, Janssens IA, Kleber M, Kögel-Knabner I, Lehmann J, Manning DAC, Nannipieri P, Rasse DP, Weiner S, Trumbore SE (2011) Persistence of soil organic matter as an ecosystem property. Nature 478(7367):49–56

Stockmann U, Adams MA, Crawford JW, Field DJ, Henakaarchchi N, Jenkins M, Minasny B, McBratney AB, de Courcelles VD, Singh K, Wheeler I, Abbott L, Angers DA, Baldock J, Bird M, Brookes PC, Chenu C, Jastrow JD, Lal R, Lehmann J, O'Donnell AG, Parton WJ, Whitehead D, Zimmermann M (2013) The knowns, known unknowns and unknowns of sequestration of soil organic carbon. Agric Ecosyst Environ 164:80–99

Templer PH, Arthur MA, Lovett GM, Weathers KC (2007) Plant and soil natural abundance delta N-15: indicators of relative rates of nitrogen cycling in temperate forest ecosystems. Oecologia 153(2):399–406

Turner BL, Condron LM, Wells A, Andersen KM (2012a) Soil nutrient dynamics during podzol development under lowland temperate rain forest in New Zealand. Catena 97:50–62

Turner BL, Wells A, Andersen KM, Condron LM (2012b) Patterns of tree community composition along a coastal dune chronosequence in lowland temperate rain forest in New Zealand. Plant Ecol 213(10):1525–1541

Turner BL, Wells A, Condron LM (2014) Soil organic phosphorus transformations along a coastal dune chronosequence under New Zealand temperate rain forest. Biogeochemistry 121(3):595–611

Unkovich M (2013) Isotope discrimination provides new insight into biological nitrogen fixation. New Phytol 198(3):643–646

Vitousek P (2004) Nutrient cycling and limitation: Hawai'i as a model system. Princeton University Press, Princeton

Vitousek PM, Farrington H (1997) Nutrient limitation and soil development: experimental test of a biogeochemical theory. Biogeochemistry 37(1):63–75

Vitousek PM, Howarth RW (1991) Nitrogen limitation on land and in the sea: how it can occur? Biogeochemistry 13(2):87–115

Vitousek PM, Field CB, Matson PA (1990) Variation in foliar $\delta^{13}C$ in Hawaiian *Metrosideros polymorpha*: a case of internal resistance? Oecologia 84(3):362–370

Vitousek PM, Menge DNL, Reed SC, Cleveland CC (2013) Biological nitrogen fixation: rates, patterns and ecological controls in terrestrial ecosystems. Philos Trans R Soc Lond B Biol Sci 368(1621):20130119

Walker TW, Syers JK (1976) The fate of phosphorus during pedogenesis. Geoderma 15(1):1–19

Wallander H, Morth CM, Giesler R (2009) Increasing abundance of soil fungi is a driver for N-15 enrichment in soil profiles along a chronosequence undergoing isostatic rebound in northern Sweden. Oecologia 160(1):87–96

Wardle DA, Walker LR, Bardgett RD (2004) Ecosystem properties and forest decline in contrasting long-term chronosequences. Science 305(5683):509–513

Wells A, Goff J (2007) Coastal dunes in Westland, New Zealand, provide a record of paleoseismic activity on the Alpine fault. Geology 35(8):731–734